



HAL
open science

Fabrication of bicontinuous double networks as thermal and pH stimuli responsive drug carriers for on-demand release

Clément Bombonnel, Cedric Vancaeyzeele, Gerald Guérin, Frederic Vidal

► **To cite this version:**

Clément Bombonnel, Cedric Vancaeyzeele, Gerald Guérin, Frederic Vidal. Fabrication of bicontinuous double networks as thermal and pH stimuli responsive drug carriers for on-demand release. *Materials Science and Engineering: C*, 2020, 109, pp.110495. 10.1016/j.msec.2019.110495 . hal-03093341

HAL Id: hal-03093341

<https://cyu.hal.science/hal-03093341>

Submitted on 21 Jul 2022

HAL is a multi-disciplinary open access archive for the deposit and dissemination of scientific research documents, whether they are published or not. The documents may come from teaching and research institutions in France or abroad, or from public or private research centers.

L'archive ouverte pluridisciplinaire **HAL**, est destinée au dépôt et à la diffusion de documents scientifiques de niveau recherche, publiés ou non, émanant des établissements d'enseignement et de recherche français ou étrangers, des laboratoires publics ou privés.



Distributed under a Creative Commons Attribution - NonCommercial 4.0 International License

Fabrication of bicontinuous Double Networks as Thermal and pH Stimuli Responsive Drug Carriers for On-Demand Release

Clément Bombonnel^a, Cédric Vancaeyzeele^{a*}, Gerald Guérin^b, Frédéric Vidal^a.

^a Laboratoire de Physicochimie des Polymères et des Interfaces (LPPI – EA 2528), I-Mat, Université de Cergy-Pontoise, 5 mail Gay-Lussac, 95031 Cergy-Pontoise, France.

^b Shanghai Key Laboratory of Advanced Polymeric Materials, School of Materials Science and Engineering, East China University of Science and Technology, Shanghai, 200237, China

Declaration of interests

The authors declare that they have no known competing financial interests or personal relationships that could have appeared to influence the work reported in this paper.

Abstract.

The fabrication, via a two steps approach, of a novel bicontinuous Double Network (BCDN) material is reported. We first use a bicontinuous emulsion as template to obtain a poly(butyl acrylate) (PBA) and poly(acrylic acid) (PAA) bicontinuous amphiphilic material. The material is then swollen with the precursor of a second hydrophilic polymer (PNIPAM, poly(N-isopropylacrylamide)). After polymerization of these precursors, the two responsive polymers, PNIPAM and PAA, form a double-network within a bicontinuous templated material, i.e. a bicontinuous double network (BCDN) material. The advantages of using such unique and complex double network architecture are manifold. PBA increases the mechanical properties of the hydrogel all together with the hydrophilic double network that also decouples the pH and temperature responsiveness. Among different possible applications, we tested this responsive hydrogels for its biomedical application. It can be used as pH and temperature sensitive devices for on-demand drug delivery. In addition, the release of a drug confined in the amphiphilic bicontinuous structure follows different kinetics profiles, depending on pH and temperature. This last result indicates that it is possible to control and regulate the release of an encapsulated drug according to the fluctuations of physiological conditions.

Keywords.

Soft template; Double Network; Bicontinuous microemulsion; pH and temperature responsiveness; Drug release

1. Introduction

“Smart” hydrogels are three-dimensional networks having the ability to reversibly swell/deswell in water in response to an external stimulus such as a change in pH or temperature, or the application of a magnetic/electric field.[1] Temperature and pH are stimuli among the most studied, especially in the area of drug release. Due to their stimuli-responsive abilities, “smart hydrogels” could potentially deliver an encapsulated molecule according to physiological conditions. Controlled release of drugs from a scaffold can accelerate the local therapeutic process. It by-passes undesired side effects of a drug that are amplified because of overexposure. At the same time, the drug concentration has to be above a threshold to be effective, with a relevant dose of drug at the targeted site for an extended period of time. Hence, smart hydrogels are suitable carriers for delayed release drug delivery.[2,3]

Smart hydrogels are usually made of copolymers containing at least one stimuli-responsive group. The most commonly used thermosensitive polymer is poly(N-isopropylacrylamide) (PNIPAM) because it undergoes a volume phase transition at a temperature (VPTT, 32°C) close to that of the human body.[4,5] PNIPAM is often copolymerized with a polyelectrolyte to produce a material also sensitive to pH.[6,7] Polyelectrolytes are mainly poly(carboxylic acid) based polymers because their pKa are in the pH range of different human organs. However, copolymerization of NIPAM with an ionisable co-monomer increases its hydrophilic character. The thermal-response of the copolymers can thus drop drastically, especially when the polyacid is fully ionized. The offset of the lower critical solution temperature (LCST) is shifted to higher temperatures as more energy is required to break the hydrogen bonds.[6–8] To overcome this problem, Gong *et al.* used another type of hydrogel[9], called double network (DN) with mechanical properties that are considerably superior to those of conventional hydrogels.[9–11] The DN is defined as the combination of two networks: the first network is a rigid and brittle polyelectrolyte, densely crosslinked while the second network is composed of a neutral polymer, soft, ductile and loosely crosslinked. The molar concentration of the second network is 20-50 times higher than that of the first one, and the overall structure forms a material whose networks are strongly interpenetrated, but not chemically attached. A DN of PNIPAM and poly(carboxylic acid)[12,13], thus does not show any sign of the mutual interference[14,15] described above.

Recently, we have demonstrated the asset of the confinement of PNIPAM within a bicontinuous (BC) amphiphilic structure generated by microemulsion soft templating on delaying drug release.[16] The hydrophobic scaffold and hydrophilic drug reservoir domains were entangled, slowing down the drug desorption. In addition to the inherent tortuosity of the bicontinuous structure, a scaffold with a low glass transition temperature (Tg) could expand when the hydrogel collapsed. In the collapsed state, this hydrophobic scaffold would

cover the surface of the hydrogel, burying the hydrophilic PNIPAM network, and reducing the exchange surface area with the aqueous medium, as well as the drug [release](#) rate.

Here, we describe a new strategy to prepare polymeric drug carriers that would release the drug “on-demand” according to changes in physiological conditions. While DN hydrogels appear to be excellent candidates for drug delivery purpose, due to their multiple stimuli-responsive properties, they still suffer from a fast release rate of the encapsulated drugs, failing to prevent the burst effect. To overcome this issue, we have chosen to confine a PNIPAM/PAA DN inside a bicontinuous structure. These materials, named bicontinuous double network (BCDN), are amphiphilic bicontinuous hydrogels with a hydrophobic phase composed of PBA and a hydrophilic phase composed of a PNIPAM+PAA double network. In this way, the double PNIPAM+PAA network, which serves as drug reservoir, is confined within a hydrophobic environment. In this paper, the specific confinement offered by the bicontinuous structures leads to the formation of hydrogels that possess the stimuli-responsive properties of each partner of the DN, while limiting their usual burst effect.

2. Experimental Section

Chemicals. N-isopropylacrylamide, (NIPAM, 97%), N,N-methylenebisacrylamide, (MBA, 99%), ethylene glycol dimethacrylate (EGDMA, 98%), isocyanatoethyl methacrylate ICEMA (98%), dibutyltin dilaurate (DBTDL, 95%), acetylsalicylic acid (ASA, 99%), and poly(oxyethylene) (n = 23) lauryl ether (Brij 35, 99%) were provided by Sigma-Aldrich and were used as received. Acrylic Acid (99.5%) was provided by Acros Organics. Butyl acrylate (BA, Sigma-Aldrich) was distilled before use. 2-Hydroxy-2-methylpropiophenone (Darocur 1173, D₁₁₇₃, Ciba), 1-[4-(2-hydroxyethoxy)-phenyl]-2-hydroxy-2-methyl-1-propane-1-one (Irgacure 2959, I₂₉₅₉, 98%, Sigma-Aldrich), tetrahydrofuran (THF, VWR), were used as received. Water was deionized through a MilliQ purification system before use.

Instrumentation.

Photopolymerization for the synthesis of single networks, bicontinuous materials and “bicontinuous double networks” was performed under a UV curing lamp (Primarc UV Technology, Minicure, Mercury vapor Lamp, 100W cm⁻¹).

Fourier transform infrared (FTIR) spectroscopy was performed on a Bruker spectrometer (Equinox 55) by averaging 16 consecutive scans with a resolution of 4 cm⁻¹. The rates of the network formation in the bulk were followed by monitoring in real time the disappearance of the H–C=C overtone absorption bands at 6190 cm⁻¹ for NIPAM, 6180 cm⁻¹ for AA and 6160 cm⁻¹ for BA. A given peak area is directly proportional to the reagent concentration (the Beer–Lambert law has been verified); thus, the conversion-time profile can be easily derived from the spectra recorded as a function of time. The conversion of reactive bonds was calculated as $p = 1 - (A^t/A^0)$ from the absorbance values, where A is the absorbance, and the superscripts 0 and t denote the reaction times, i.e., the time of exposure of the materials to

the UV curing lamp. The materials were synthesized in a mold made of two glass plates clamped together and sealed with a 1 mm thick Teflon gasket.

The ultraviolet–visible (UV–vis) spectra were recorded in a Suprasil cell (pathlength 10 mm, Hellma) on a V570 spectrometer (Jasco) in the transmission mode with a 2 nm bandwidth at 400 nm min⁻¹.

¹H and ¹³C NMR spectra were recorded with a Bruker DPX250 spectrometer in CDCl₃ as the solvent and reference. All chemical shift values are given in ppm.

Rheological measurements were performed with an Anton Paar Physica MCR 301 rheometer equipped with a CTD 450 temperature control device and a cone–plate geometry (cone: diameter 25 mm, angle 2°; plate: polymerization system made from glass coupled with UV Source Omnicure). A 0.5% deformation was imposed at 1 Hz. The storage modulus (G′) and loss modulus (G″) were recorded as a function of time. The gel time was determined at the intersection between the storage and loss modulus curves. The solution of the precursors was put in the geometry, and measurement began immediately with UV exposure (Hg vapor lamp, 19 W cm⁻²) at 25 °C. Data were acquired with the Rheoplus v3.40 software.

Dynamic mechanical analysis (DMA) was performed using a Q800 apparatus (TA instruments). Experiments were carried out from -80°C to 200°C with a 3°C min⁻¹ heating rate and a constant 1 Hz frequency. The hydrogel moduli were measured after 7 days of immersion in DI water at room temperature at 1Hz and 0.05% deformation in tensile mode.

Optical microscopy imaging was performed with crossed polarizers (U-AN360/U-PO) on an Olympus BX60M microscope with UMPlan FI objective (10x/0.3 BD). Microemulsions and hydrogels were imaged by confocal laser scanning microscopy (CLSM) (LSM 710, Zeiss, Germany) using the ZEN2010 software. 9,10-Diphenylanthracene (DPA, Acros, 99%; 0.3wt %) and rhodamine B (RB, Aldrich; 0.04 wt %) were dissolved before emulsification in the organic and aqueous phases, respectively. For the fluorescence contrast method, excitation wavelengths were 405 nm (30 mW, emission window from 420 to 460 nm) and 561 nm (20 mW, emission window from 570 to 640 nm). These measurements were performed with a plan-apochromatic objective (63x/1.40 oil immersion). Each line was scanned and averaged four times with a field resolution of 1024 × 1024 pixels and a 16 bit dynamic range. The selected images were obtained by focusing in the bulk of the samples.

Scanning transmission electron microscopy was carried out on a ZEISS Gemini SEM 300 on cryo-microtomed samples (thickness ~50 nm). OsO₄ was used as contrast agent for staining the hydrophilic phase of the materials.

Differential scanning calorimetry (DSC) was performed on a DSC Q100 model (TA Instruments). The thermograms were recorded at a heating rate of 10 °C min⁻¹ between -90 and 150 °C. Between the first and the second scan, the sample temperature was decreased at a rate of -10 °C/min to favor any possible crystallization. Thermal transitions were detected on the second scan.

The soluble fractions (SFs) contained in the dried materials were removed in a Soxhlet extractor using THF. After 72h of extraction, the sample was dried again under vacuum at 40 °C until a constant weight was established. The SF was determined as a weight percentage: $SF(\%) = \frac{(W_0 - W_t)}{W_0} \times 100$, where W_0 and W_t are the sample weights before and after extraction, respectively. The SFs were then analyzed by 1H NMR using a Bruker Avance DPX250.

To determine the water uptake (WU) of the samples, the as-prepared gels were first immersed in buffer solution at pH = 2 and 7.8 at constant temperature for 24 h. The sample weights were, then, measured (w_1) and the samples were dried until a constant weight (w_2) was obtained. The WU was calculated as $WU(\%) = (w_1 - w_2)/w_2 \times 100$. For drug loading experiments, the polymer sample was dried and weighted (w_{polymer}) after Soxhlet extraction. It was, then, immersed for 24 h at 25 °C in an ethanol solution containing ASA ([ASA] = 150 g/L). Then, the sample surfaces were wiped, and the loaded sample was dried until constant weight ($w_{\text{polymer+drug}}$). The weight ratio of ASA absorbed was calculated as $\%loading = (w_{\text{polymer+drug}} - w_{\text{polymer}})/w_{\text{polymer}} \times 100$.

The drug release from ca. 0.2 g of the material was monitored in buffered water solution at pH = 2 or 7.8 and at 25 or 40°C. To determine the release kinetics, the ASA-loaded materials were immersed in a large volume of buffer solution. The cumulative molar concentration of ASA in water was determined by UV titration at 275 nm using an external standard calibration curve with $Abs_{(275 \text{ nm})} = 218.02 [ASA]$. The cumulative weight percentage of ASA extracted from the material was calculated from this concentration and the drug loading percentage.

Surfmer Synthesis from Brij 35. Dried Brij 35 (10 g, 8.35mmol) was dissolved under magnetic stirring in 35 mL dichloromethane, previously distilled and dried on calcium hydride, in a 100mL two-neck round-bottom flask connected to a condenser. The solution was purged under argon before addition of 105 mg DBTDL (0.17 mmol; 1 mol % with respect to ICEMA; 98.5 μ L). Then, 2.6 g of ICEMA (16.7 mmol; 2.36 mL) was added dropwise and the solution was stirred for 3 h at 25 °C. The product was washed by precipitation in diethyl ether, dried, and stored under vacuum. 1H NMR in $CDCl_3$: 0.75 (t, CH_3 al), 1.18 (m, CH_2), 1.85 (s, CH_3 -C=C), 3.39 (m, CH_2 (al)-O), 3.57 (m, CH_2 - CH_2 -O), 3.64 (m, CH_2 - CH_2 -OCO), 4.14 (m, CH_2 -OCO), 5.5 (1H, s, CH_2 =C) and 6.01 ppm (1H, s, CH_2 =C). ^{13}C NMR in $CDCl_3$, δ (ppm) = 158.3 ppm (C=O, urethane), 166.8 ppm (C=O, methacrylate). FT-IR: ν 1716 cm^{-1} : C=O_{ester}, ν 1096 cm^{-1} O=C-O-R_{ester}, ν 1635 cm^{-1} : C=C and no ν 2270 cm^{-1} : NCO

Polymerization in Microemulsion. The microemulsion structure depends on the proportions of the aqueous phase, the surfactant, and the organic phase. By analogy with a previous study,[16] the weight percentages of aqueous phase (Φ_{aq}), surfactant and organic phase were set to $\Phi_{aq}/\text{surfactant}/\Phi_{org} = 46/38.6/15.4$. 0.772 g Brij35_{surf} was dissolved at room temperature in the organic phase, composed of 0.293 g PBA and 15 mg EGDMA degassed under argon. Emulsification was carried out by the addition under hand stirring of the

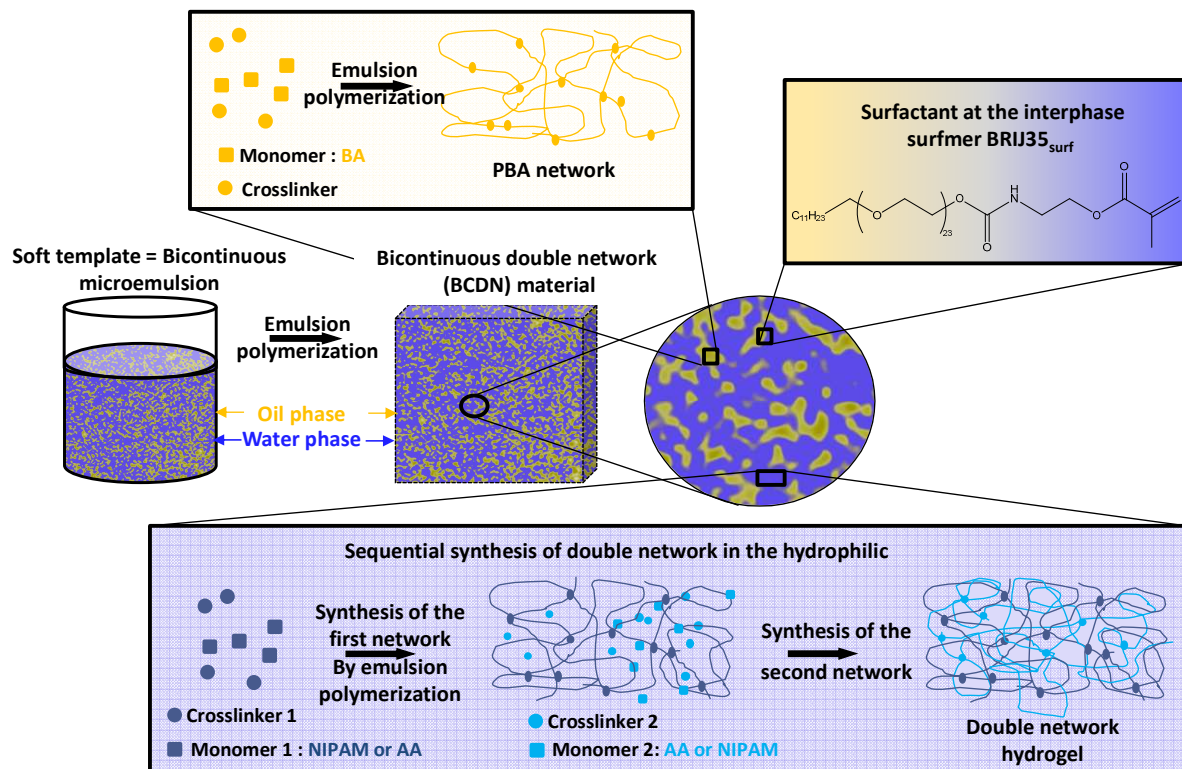
aqueous phase composed of 0.138 g of monomer (AA or NIPAM) and 9 mg MBA previously dissolved in 0.772 g deionized water degassed under argon. Radical polymerization was performed in the microemulsion by adding 6 mg D₁₁₇₃ to the organic phase at RT before emulsification, while the photopolymerization was done by pouring the microemulsion into the previously described mold and exposing it to UV irradiation for 1 min. Transparent samples were obtained. After synthesis, these samples contained mainly water, and needed to be dried under vacuum until they reached a constant weight before to be characterized and used for the preparation of the bicontinuous double network sample.

Bicontinuous Double Network Synthesis. The “bicontinuous double network”, BCDN, was prepared from the bicontinuous material through a two-step polymerization. The PNIPAM/PBA or PAA/PBA was immersed in a solution of AA (2M, buffered to pH = 1) or in a solution of NIPAM (1M, buffered to pH = 9), respectively. Each precursor solution contained a mass ratio of crosslinker (MBA) to monomer equal to 3 wt% and mass ratio of I₂₉₅₉ to monomer equal to 1 wt%. After the equilibrium state was reached, the swollen samples were wiped to remove the excess of solution at the surface, and then delicately placed between glass plates. The mold was irradiated for 1 min to initiate the polymerization of the AA or the NIPAM respectively into the PNIPAM network or the PAA network.

These BCDNs will be noted [PNIPAM+PAA]/PBA or [PAA+PNIPAM]/PBA. The bicontinuous material (first step of synthesis) is composed of an hydrophobic polymer (outside the bracket) and an hydrophilic polymer (right-hand side inside the bracket) while the third polymer of the double network (second step) is on the left-hand side inside the bracket. For example, in the case of [PNIPAM+PAA]/PBA, the bicontinuous material is made of PBA and PAA, while PNIPAM is used for the second network.

3. Results and discussion.

In this paper we describe the fabrication of an original macromolecular architecture in which two responsive polymers, PNIPAM and PAA, form a double-network within a bicontinuous templated material, i.e. a bicontinuous double network (BCDN) material. There are few successive steps that are required to obtain such structures (Scheme 1), each of them offering their own challenges.



Scheme 1: Structuration of the bicontinuous double network (BCDN). It is an amphiphilic bicontinuous hydrogel with a hydrophobic polymer network and a hydrophilic phase composed of a double network hydrogel.

First, one needs to prepare the oil/water bicontinuous microemulsion (Winsor IV emulsion) that would be used as template for the bicontinuous structure. Soft templated materials by bicontinuous emulsions are different from polymer blend or [interpenetrating polymer networks](#) (IPNs), because they are not synthesized from a homogeneous solution composed of all the starting products mixed together (i.e. monomer, oligomer, cross-linkers, catalyst and initiator) with an uncontrolled phase separation occurring during polymerization. Hence, the material morphology is predetermined before polymerization. However, maintaining the microemulsion structure during the polymerization can also prove extremely difficult, because it is altered by changes in temperature and composition. Indeed, polymerization in bicontinuous microemulsion often results in the modification of the interphase curvature, leading to a phase rearrangement that disrupts the bicontinuous structure. If the newly-formed polymer phases are not efficiently stabilized by the surfactant, they can flocculate and form micrometer-sized aggregates.[17,18] There are only few reports [on](#) the successful preparation of microemulsion templated bicontinuous structures. [Those structures were](#) only observed when the monomer in one of the phases of the microemulsion [was](#) simultaneously polymerized and cross-linked.[19–21] Chew *et al.* have shown that the microemulsion structure [could](#) be preserved by using polymerizable surfactant and [carried](#) out at a fast polymerization rate which freezes the system.[22–25] Gan *et al.* were among the first [groups](#) to describe [the formation of](#) bicontinuous materials templated by

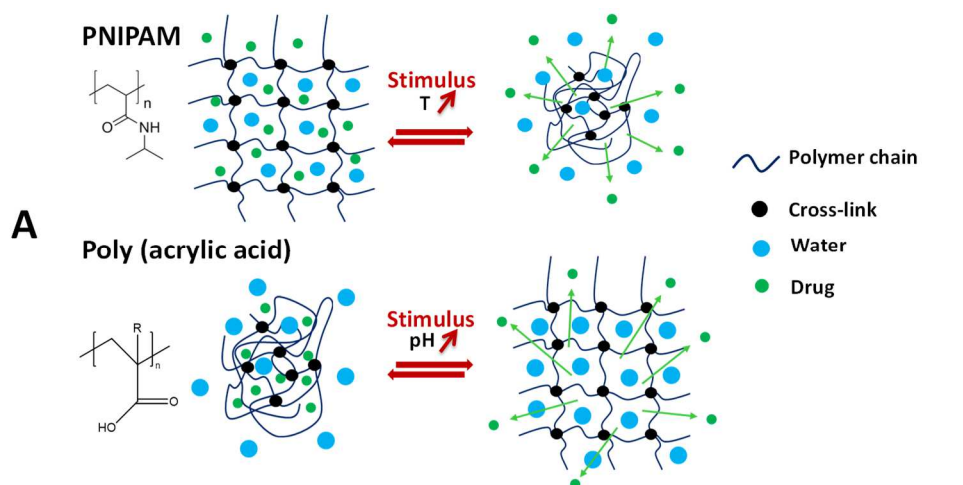
microemulsion with monomers polymerized and cross-linked in both phases.[26–28] More recently, we have also reported the synthesis of bicontinuous materials with hydrophilic polymer domains entangled with continuous hydrophobic polymer domains.[16] The dual phase continuity[29] was imposed by the bicontinuous microemulsion used as a soft template.[30,31]

Taking the preparation of this bicontinuous structure as an asset, we decided to develop a more complex system by incorporating a second network inside the bicontinuous phase. We chose to prepare a BCDN, which would preserve the main characteristics of the two networks. While the final structure was relatively complex, the protocol followed to generate it was surprisingly simple (Scheme 1). Once the bicontinuous single network was formed, the newly formed material was soaked into a solution of the hydrophilic precursor of the second network. This second step is analogous to the Gong's protocol developed for classical DN hydrogels.[9] Fast polymerization of the second monomer then led to the formation of a second network within the first hydrophilic one. In the following sections, we are answering some key questions related to the preparation of this novel structure. For example, does the addition of a second network induce a microphase separation? Is the second network strictly located in the hydrophilic network, and can it be polymerized at high yield? Can we still obtain a BCDN if we inverse the order of synthesis of the two stimuli-responsive hydrophilic networks and how does that affect their final properties? To answer this last question, we decided to investigate a very simple system by following the release of ASA from the newly synthesized BCDN at different thermal and pH stimuli.

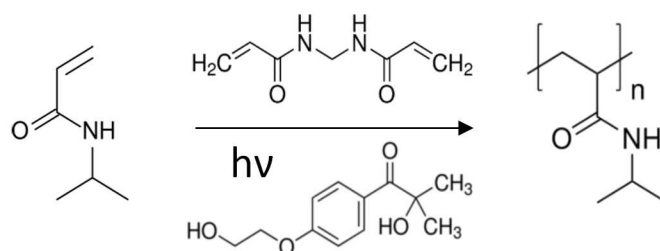
3.1. Responsive Polymers partners

We wanted to prepare an encapsulating BCDN material able to regulate the drug release. The regulation has, thus, to be controlled with physiological parameters that vary within the human body. From a biomedical point of view, the drug carrier has to be sensitive to the temperature and/or pH of the surroundings. Thermal sensitive systems may be useful in transdermal-type delivery device. The successive heating and cooling of the device, around its LCST and within the range of physiological temperature, results in pulsatile drug release.[32] *In vivo*, temperature controlled drug release has also been explored for the delivery of anti-cancer drugs.[33] Cancer cells are less resistant to heat than normal cells and are weakened over 42.5 °C. Cancerous tumors can thus be treated using, or in combination with, thermo-responsive polymeric carriers that release the drugs once heated above 42.5 °C.[34] Besides, pH sensitive systems may be useful for oral delivered medicine. The drug carrier should protect the drugs from degradation in gastric acid[35], when the drug is delivered orally, and permit the deliverance in neutral to basic medium. The drug will have a higher probability to efficiently pass through the gastrointestinal mucosal barrier if the smart polymer carrier delivers the drug over a long period of time, with negligible burst effect, at the basic neutral gastrointestinal pH.[36] Indeed, human body exhibits variations of pH along the gastrointestinal tract, and also in some specific tissues (and tumoral areas) and sub-cellular compartments.

The two stimuli-responsive polymers selected are PNIPAM and PAA. PNIPAM is a thermosensitive polymer (Figure 1A). When the temperature is elevated above the LCST of 32°C, close to the body temperature[4], the hydrogen bonds with water break and the PNIPAM undergoes a reversible VPTT from a water swollen state to a hydrophobic and collapse state. Thus, a drug loaded PNIPAM hydrogel shrinks above the LCST, expelling both the drug and water molecules.[37] Such phase transition can potentially be used to control drug-release and achieve pulsatile on–off drug release in response to temperature fluctuation around the PNIPAM LCST.[32,38,39]



PNIPAM Poly(N-isopropylacrylamide) network



PAA Poly(acrylic acid) network

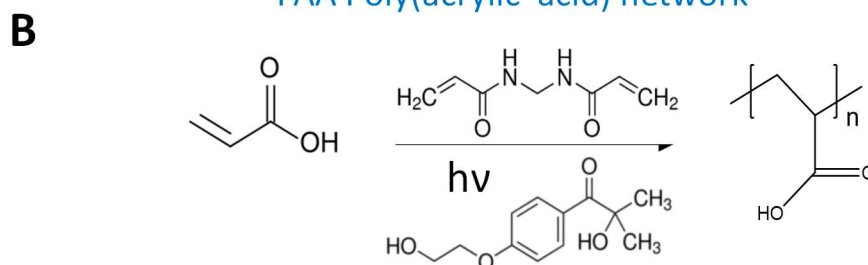


Figure 1: Stimuli responsive polymer network. A: schematic representation of the drug release mechanism under temperature or pH stimulus. B: Photopolymerization/cross-linking reaction during PNIPAM and PAA network formations.

The pH responsive polymer used for this study was PAA. In drug release literature, PAA is considered a pH-sensitive barrier.[39] A rapid release occurs under neutral/basic conditions

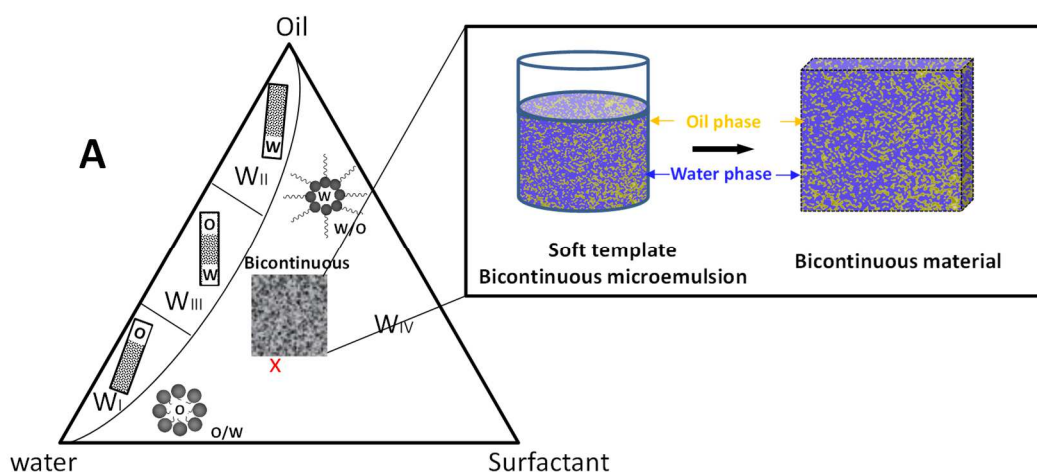
as the hydrogel passes down the intestinal tract. Briefly, the carboxylic groups of PAA are protonated at acidic pH ($pK_a = 4$) and ionized at neutral to basic pH. The presence of ionizable weak acidic moieties attached to a hydrophobic backbone triggers chain transition from a globule ($pH < 4$) to a coil ($pH > 4$) states, induced by the electrostatic repulsions of the generated charges (Figure 1A).

First we synthesized these common networks, such as single network, double network and co-networks ([network of PAA-co-PNIPAM copolymer](#)) to be used as control samples. Their full characterizations are reported in supporting information (Figure S1, S2 and S3).

3.2. Bicontinuous templated amphiphilic materials

As described earlier, one of the key step of the synthesis of BCDN material is to prepare the bicontinuous microemulsion used as soft template.

The microemulsion structure, at a given temperature, is governed by the proportion of the aqueous and organic phase (Figure 2A). The appropriate composition of the different phases for the bicontinuous structure is imposed by the weight proportions of the aqueous phase (46 wt%), the hydrophobic phase (15.4 wt%) and surfactant (Brij35_{surf}, 38.6 wt%).^[17,40] In this study, the two phases [were](#) stabilized by a polymerizable surfactant, *i.e.* a surfmer (Figure 2B). The surfmer [preserved](#) the bicontinuous structure during the reaction and [reduced](#) the risk of desorption when the samples [were](#) in an aqueous medium.^[41,42] This surfmer is noted as Brij 35_{surf} and its synthesis has been described previously.^[16] To preserve the main features of the bicontinuous microemulsion template, we synthesized the different networks by photopolymerization, a technique that favors fast polymerization/crosslinking reactions at moderate temperatures.^[43] In this architecture, the hydrophilic polymer domains [were](#) entangled with the hydrophobic polymer partner (PBA) after concomitant polymerization (Figure 2C). PBA is a soft polymer with a low glass transition temperature (T_g) of $-43\text{ }^\circ\text{C}$ and a modulus of 11 MPa at room temperature. In addition, PBA is not cytotoxic and biocompatible.^[44–48]



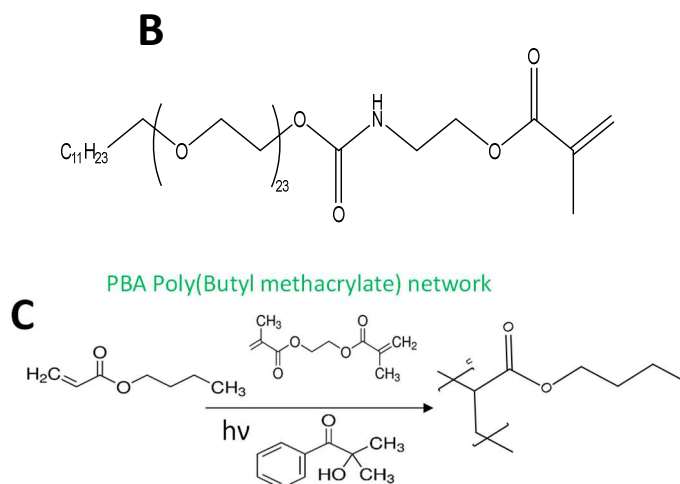


Figure 2: (A) Schematic representation of an Oil/water/surfactant ternary diagram displaying Winsor type emulsion according to composition. Winsor IV emulsions can form either oil in water (O/W), water in oil (W/O) or bicontinuous microemulsions. (Note: X represents the selected microemulsion composition). Scheme of the soft templating of bicontinuous material. (B) Chemical formula of the surfmer BRIJ35_{surf}. (C) Photopolymerization/cross-linking reaction during PBA network formation.

3.2.1. PNIPAM/PBA BC materials

The PNIPAM/PBA bicontinuous material was synthesized in a bicontinuous microemulsion,[16] that ensured the co-continuity of the two polymer domains. With this morphology, the properties of the immiscible polymers are usually better combined.[49–51] The aqueous phase of the microemulsion was composed of the precursor of PNIPAM single network and the hydrophobic phase with those of the PBA network. The photopolymerization, initiated by Darocure 1173 under UV irradiation, was monitored by FTIR in the near IR region. The reactive function consumption was complete within 60s (Figure S4). From the small amount of polymer recovered (3%) by Soxhlet extraction, we concluded that PBA and PNIPAM were cross-linked.

Similarly to the bicontinuous microemulsion template, the PNIPAM/PBA bicontinuous material was transparent (Figure 3A). No birefringence was observed (not shown), which is typical of anisotropic structures.[17] To evaluate how the aqueous and organic phases were mixed, we studied both the PNIPAM/PBA microemulsion template and the material obtained after photopolymerization by confocal laser scanning microscopy (CLSM) was used to. For this effect, we introduced 9,10-diphenylanthracene (a fluorescent dyes only soluble in the organic phase), and rhodamine B (soluble in the aqueous phase) before emulsification. As shown in Figure 3B, one cannot observe any sign of large-scale demixion in the microemulsion template. After photopolymerization, CLSM images (Figure 3B) of the resulting hydrogel confirmed the absence of demixion during polymerization because the

dyes, strictly soluble in hydrophilic or hydrophobic domains, remained co-located. These images are different from that of Castellino *et al.*[52] who used bicontinuous microemulsion to structure interpenetrating polymer networks (IPN) before synthesis. By copolymerizing a silicone acrylate surfactant with the monomer in the aqueous phase, the authors could successfully preserve the bicontinuous structure. They could unfortunately not fully prevent microphase separation to occur, as observed by optical microscopy. This was not the case in the system presented here.

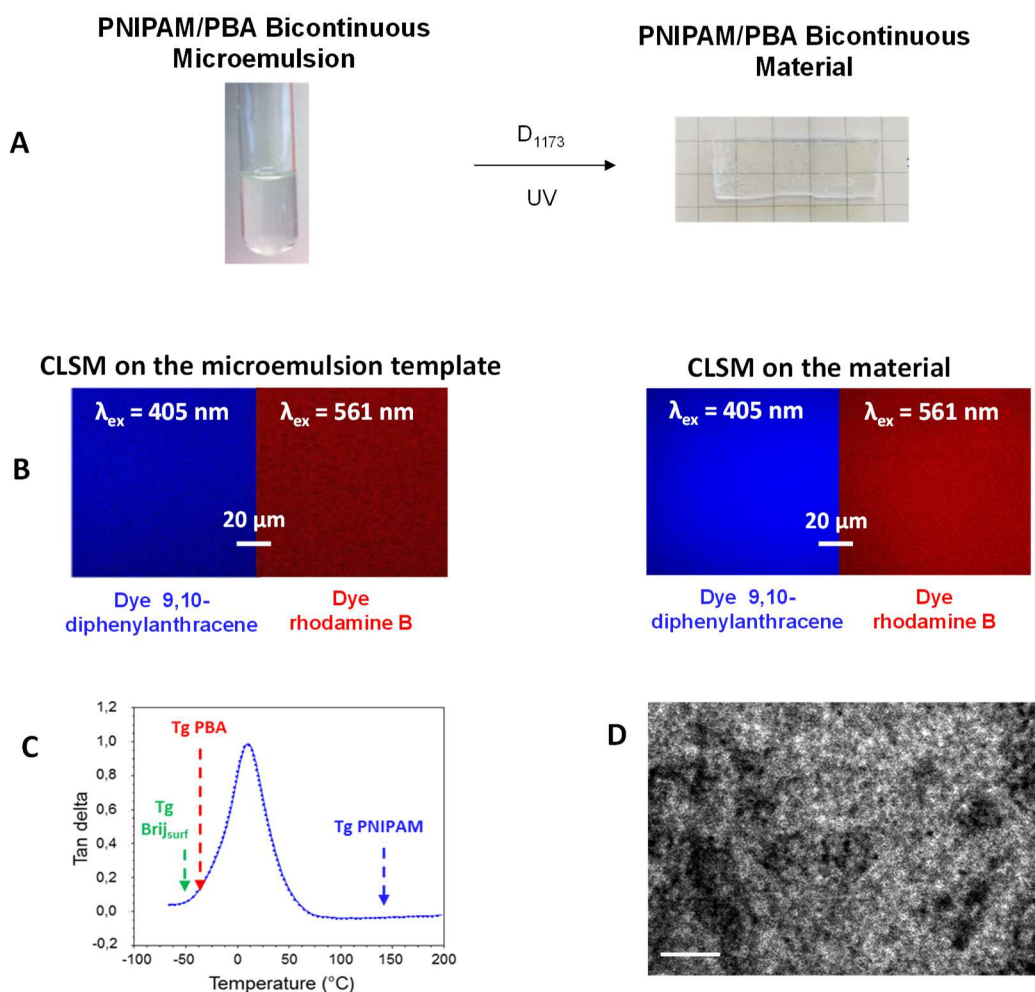


Figure 3: (A) PNIPAM/PBA bicontinuous material synthesis. (B) CLSM image of PNIPAM/PBA microemulsion template before and after photopolymerization. Selective staining of the two phases are done: Φ_{aq} stained red with RB, and Φ_{org} stained blue with 9,10-DPA. (C) Tan δ -temperature curve recorded on PNIPAM/PBA bicontinuous sample. (D) TEM image of PNIPAM/PBA bicontinuous sample with hydrophilic PNIPAM stained with OsO₄, scale bar: 200nm.

To gain a better insight into the morphology of the PNIPAM/PBA BC material, the sample was studied by DMA, specifically focusing on the evolution of tan δ as a function of temperature (Figure 3C). The dried PNIPAM single network was too brittle to be analyzed by DMA. In Figure 3C, the Tgs of the different constituents are also reported for comparison. Interestingly, a single tan δ peak is observed indicating that the BC material is homogeneous

at the DMA scale.[53] This result is somewhat surprising since the components of this material are structured through the bicontinuous microemulsion template, namely two immiscible domains stabilized by a surfactant. Therefore, one would intuitively expect the hydrophilic and hydrophobic components to relax independently at different temperatures, leading to the presence of two distinguishable $\tan\delta$ peaks. This apparent contradiction can, however, be easily resolved when one considers that the domains imposed by the bicontinuous template are relatively small (30-50 nm).[54] At such scale, hydrophilic and hydrophobic domains are tightly intertwined, and polymer chains relax at the same temperature. The TEM picture shown in Figure 3D confirms the limited phase separation arising from the soft template. The dark areas of the TEM image represent electron dense regions of the PNIPAM stained with OsO_4 . The photopolymerization in the bicontinuous microemulsion template resulted in small PNIPAM domains (dark) that appear to be intertwined with PBA domains (white). It shows the typical pattern observed in a bicontinuous microemulsion with entangled and co-continuous hydrophilic and hydrophobic phases.[55]

The next step was to bring pH-sensitivity to this thermo-responsive BC material by the addition of a PAA network.

3.2.2. [PAA+PNIPAM]/PBA BCDN materials

Following the literature on the preparation of PAA+PNIPAM double networks[12,13], [PAA+PNIPAM]/PBA BCDN samples were synthesized according to the reverse method of DN synthesis, where the first network is a neutral polymer and the second network is a polyelectrolyte. The first network formed (in the present case, PNIPAM/PBA BC) was immersed in an aqueous solution containing the PAA precursor (AA, cross-linker and initiator), and buffered to $\text{pH} = 1$. The second network was then obtained after photopolymerization of AA as described in Figure 4A. To insure that the aqueous phase containing AA would only swell the hydrophilic phase of the PNIPAM/PBA bicontinuous material, we first measured the amount of swelling of a PBA single network immersed in the solution of the PAA precursor. As expected, the swelling ratio of PBA did not exceed 6%, a clear indication that the hydrophobic phase would be hardly affected by the immersion step.

PNIPAM/PBA BC materials were, thus, immersed in the PAA precursors solution for the synthesis of [PAA+PNIPAM]/PBA BC materials. After reaching the equilibrium swollen state, the samples were wiped to remove the excess of solution and then delicately placed between glass plates. The mold was irradiated for 1 min to initiate the photopolymerization of AA within the hydrophilic phase. After polymerization, the hydrogel material remained transparent. The soluble fraction, which was extracted with THF for 72h, was limited to 6% of linear PAA. In addition, the weighing of the extracted material after drying allowed us to determine their final mass composition (Table 1). PAA weight proportion was a lot larger than that of PNIPAM.

Table 1 : Mass proportion of each polymer partner of the dry material before and after the polymerization of PAA

	Components proportion (wt%)			
	PBA	Brij _{surf}	PNIPAM	PAA
PNIPAM/PBA BC	25	63	12	-
[PAA+PNIPAM]/PBA BCDN	13.8±0.5	34.7±1.3	6.5±0.3	45±2

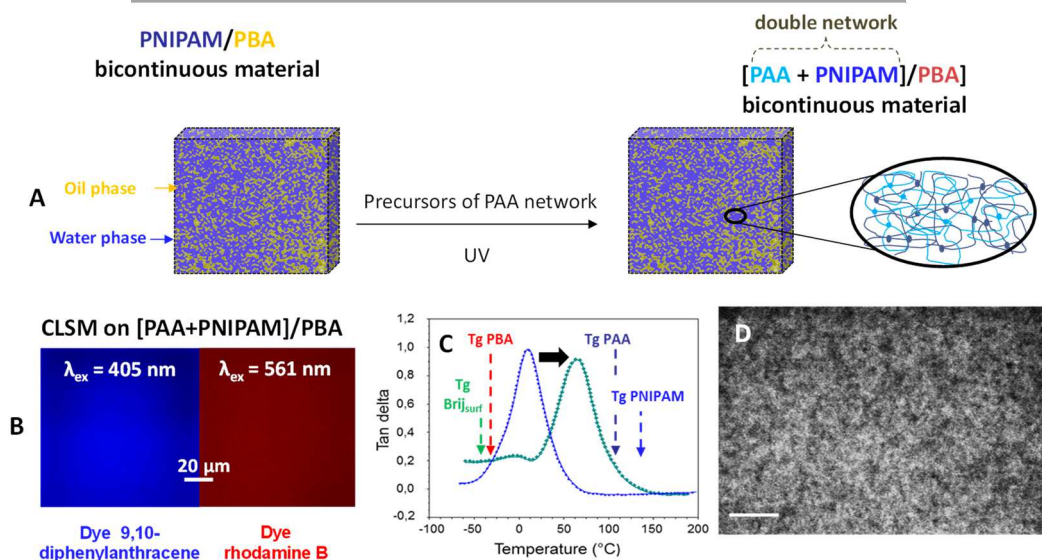


Figure 4: (A) [PAA+PNIPAM]/PBA material synthesis. (B) CLSM image of [PAA+PNIPAM]/PBA material. Selective staining of the two phases are done: Φ_{aq} stained red with RB, and Φ_{org} stained blue with 9,10-DPA. (C) Tan δ -temperature curves recorded on [PAA+PNIPAM]/PBA material. (D) TEM images of [PAA+PNIPAM]/PBA material, hydrophilic network stained with OsO₄ and scale bar: 200nm.

We were concerned that the addition of a large amount of PAA (45 wt%) into the bicontinuous structure would impact its properties and before all on the primary structure of the soft template. The CLSM image of the dyed [PAA+PNIPAM]/PBA BCDN sample shown in Figure 4B was similar to that of the PNIPAM/PBA BC network (Figure 3B), clearly indicating that the formation of the PAA network did not induce any microphase separation. We then turn our attention into the mechanical properties of the BCDN. Since PAA has a T_g of ca. 105°C,^[56] one would expect the incorporation of the PAA network to strongly affect the mechanical properties of the dry BCDN. As anticipated, the plot of tan δ versus temperature (Figure 4C) shows a strong shift towards higher temperatures from 12 to 68°C. Despite this strong shift only one main relaxation peak could be observed, indicating that the presence of PAA network into the hydrophilic phase did not induce any macro-phase separation. This result was further confirmed by the TEM imaging of a microtome section of the BCDN stained with OsO₄ (Figure 4D). Once again, one observes the typical pattern formed by bicontinuous structures, confirming that the addition of the PAA network **did not disrupt the structure**.

Figure 5 displays the water uptake (WU) of PNIPAM/PBA and [PAA+PNIPAM]/PBA BCDN, at pH = 2 and 7.8 (*i.e.* below and above the pKa of the acrylic acid functionalities) as a function of temperature from 20°C to 50°C. As expected, the incorporation of PAA increased the hydrophilic behavior of the material, shifting the plot of WU versus temperature towards higher values of WU for [PAA+PNIPAM]/PBA BCDN compared to PNIPAM/PBA. The ionization state of PAA also influenced the WU, and conferred pH sensitive properties to [PAA+PNIPAM]/PBA BCDN. WU at 20°C was *ca.* 1.5 times larger in slightly basic conditions (up to 300wt% with AA functionalities in ionic form), than in acid condition (up to *ca.* 200wt% with AA functionalities protonated). In addition, one observes that WU decreased as the temperature increased, which indicates that the BCDN is thermo-responsive. However, the evolution of WU with temperature did not show the typical change in slope inherent to the VPTT of PNIPAM, and caused by the shrinkage of PNIPAM network at its LCST. There are two possible causes to this tendency: (i) the BCDN did not prevent PAA from increasing the hydrophilicity of PNIPAM,[13] or (ii) the total amount of PNIPAM in the [PAA+PNIPAM]/PBA BCDN was too low (only 6.5 wt%) to induce a noticeable VPTT. In the latter case, the decrease of WU as temperature increased would be due to an increase in the hydrophobicity of both the Brij_{surf} PEO fragments and PNIPAM network with temperature.[57] To verify this hypothesis, a second BCDN containing a larger amount of PNIPAM was prepared.

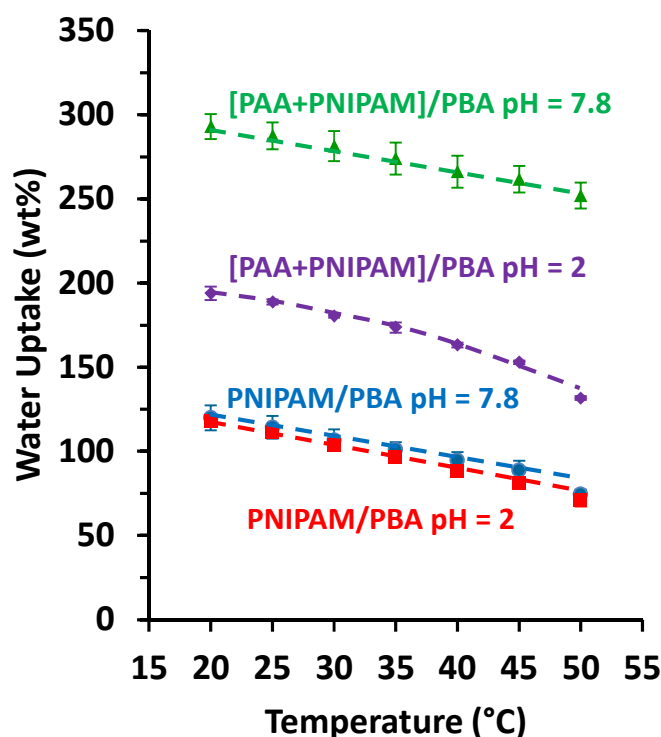


Figure 5: Water Uptake by the PNIPAM/PBA BC and [PAA+PNIPAM]/PBA BCDN as function of temperature at pH = 2 and 7.8. (The dash lines are used as guide eyes)

3.2.3. pH and temperature stimuli-responsive materials : [PNIPAM+PAA]/PBA BC material

To increase the amount of PNIPAM in our BCDN, we chose to first prepare the PAA/PBA bicontinuous network, and then to incorporate the PNIPAM. Inverting the order of formation of BCDN would not only result in an increase of the amount of PNIPAM, but it would also demonstrate the versatility of our approach.

The PAA/PBA BC material was synthesized following a similar procedure than for the synthesis of PNIPAM/PBA BC material (Figure 6A). Soxhlet extraction of this sample with THF for 72h led to a SF = 4 wt% containing a mixture of Brij_{surf} and PBA. The PAA/PBA microemulsion template and material are transparent with no birefringence (not shown) and no microphase separation could be observed by CLSM imaging (Figure 6B). The formation of a homogeneous BC morphology (at the DMA scale, *i.e.* domain size smaller than 50 nm) was also confirmed by DMA, since the evolution of $\tan\delta$ as a function of temperature showed a single peak located at $T = -15^{\circ}\text{C}$ (Figure 6C). Finally, the TEM picture presented in Figure 6D confirms that the synthesis pathway was robust as it shows the typical pattern of a bicontinuous morphology.

These results not only show that the PAA/PBA BC templated by microemulsion was obtained, but they also demonstrate that such synthesis can be done with different hydrophilic polymers.

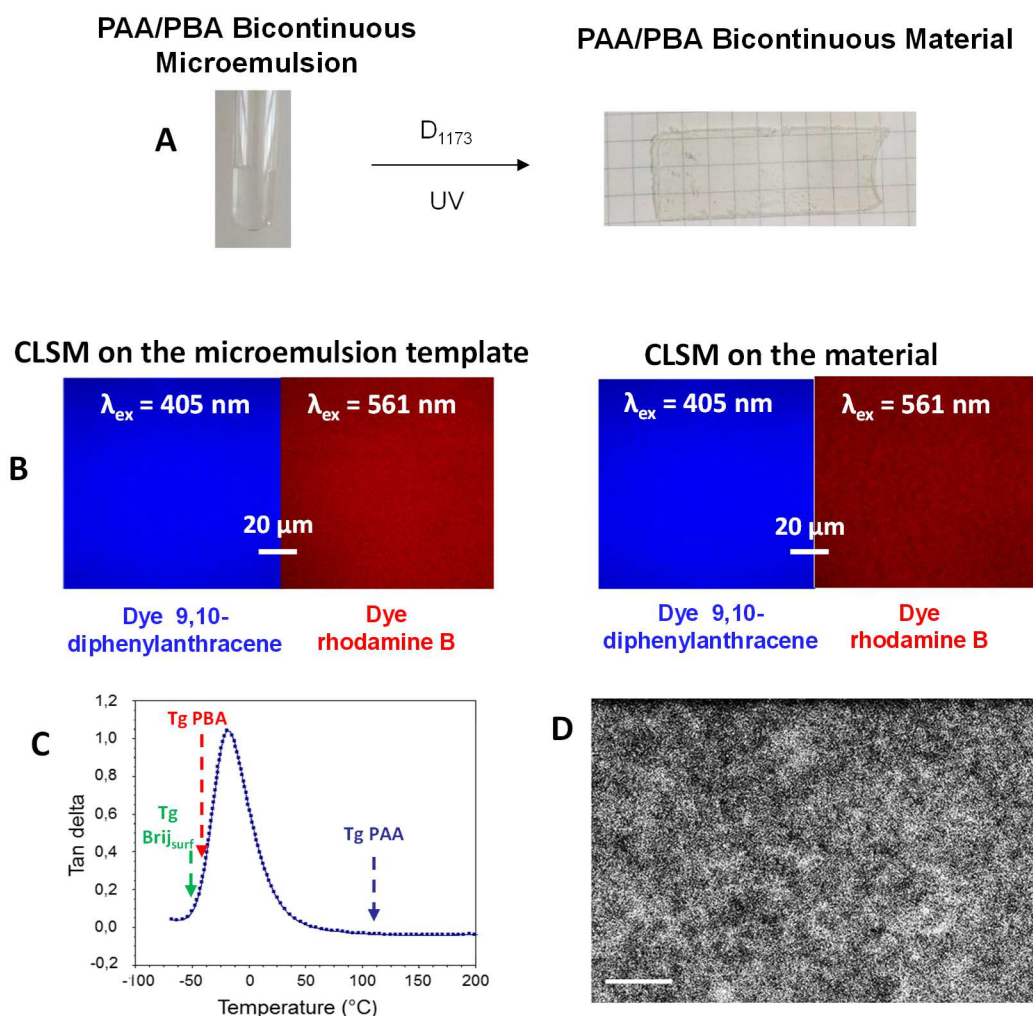


Figure 6: (A) Synthesis of the PAA/PBA bicontinuous network. (B) CLSM image of PAA/PBA microemulsion templates and PAA/PBA material. Selective staining of the two phases are done: Φ_{aq} stained red with RB, and Φ_{org} stained blue with 9,10-DPA. (C) Plot of $\text{Tan}\delta$ versus temperature performed on PAA/PBA bicontinuous network in the dry state. (D) TEM image of cryo-microtome section of PAA /PBA bicontinuous network stained with OsO_4 , scale bar: 200nm.

One of the key aspects of the formation of the BCDN is the location of the two hydrophilic networks: they have to be interpenetrated, which means that the NIPAM/cross-linker mixture as to diffuse selectively in the PAA phase. Prior to prepare the BCDN, the amount of NIPAM/cross-linker that diffused in a pure PBA network was evaluated to be lower than 2%. We could thus proceed to the second step of the BCDN formation.

The PAA/PBA BC network was immersed in buffered ($\text{pH} = 9$) aqueous solution containing the mixture of NIPAM, cross-linker and initiator. At this pH , the repulsion of electrostatic charges favored the swelling of PAA, and the diffusion of NIPAM into the PAA network was optimal. The mold containing the swollen material was irradiated under UV irradiation for 30 seconds. The soluble fraction in THF was equal to 5% and composed of linear PNIPAM, indicating that the polymerization/cross-linking was almost complete after this short

exposure time. Finally, we determined the final mass composition of [PNIPAM+PAA]/PBA BCDN (Table 2) by weighing the dried sample.

Table 2 : Weight proportion of each components of dry material before and after the polymerization of PNIPAM

	Components proportion (wt%)			
	PBA	Brij _{surf}	PAA	PNIPAM
PAA/PBA BC	25	63	12	-
[PNIPAM+PAA]/PBA BCDN	12.8±0.3	32.1±0.6	6.2±0.1	49±1

As one sees, the amount of PNIPAM present in this newly prepared BCDN has been highly increased (49%) compared to that of the previous BCDN (6%, Table 1). The co-continuous phase morphology **was preserved** during the double network formation (*i.e.* [PNIPAM+PAA]/PBA material synthesis) as shown by the TEM image in Figure 7.

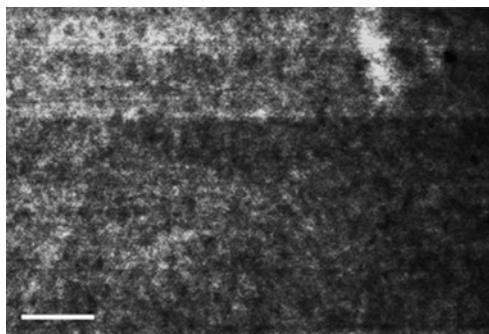


Figure 7: TEM image of [PNIPAM+PAA]/PBA BCDN. Note: the hydrophilic network was stained with OsO₄ and scale bar: 200nm.

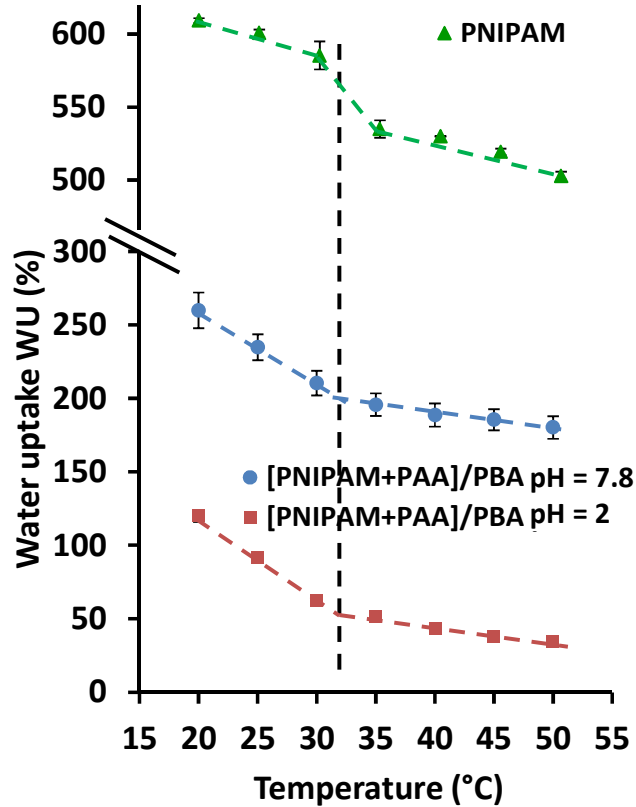


Figure 8: Water uptake of [PNIPAM+PAA]/PBA BCDN at pH = 2 and 7.8 and water uptake of PNIPAM as function of temperature. (The dashed lines are used as guide for the eyes and the error bars on the series [PNIPAM+ PAA] / PBA pH = 2 are smaller than the symbol)

The water uptake WU of [PNIPAM+PAA]/PBA BCDN as a function of temperature from 20°C to 50°C at pH = 2 and 7.8 is presented in Figure 8, along with that of the PNIPAM single network in water at neutral pH. The WU of the BCDN remains lower at pH = 2 than at pH = 7.8, indicating that the [PNIPAM+PAA]/PBA BCDN is still pH-responsive. It is worth noting that the WU of [PNIPAM+PAA]/PBA BCDN were also lower than those of [PAA+PNIPAM]/PBA BCDN at the same pHs (Figure 5, $WU_{max} = 260$ wt%, versus 300 wt% at pH = 7.8 and $WU_{max} = 120$ wt%, versus 200 wt% at pH = 2). We believe that this difference was mainly due to the change in the amount of PAA inside the BCDN since this amount decreased from 45 wt% in [PAA+PNIPAM]/PBA BCDN to 6.2 wt% in [PNIPAM+PAA]/PBA BCDN (Table 1 and 2). Interestingly, the trends of WU of [PNIPAM+PAA]/PBA BCDN as a function of temperature display a clear change in the slope in acid and basic conditions at ca. 32°C. Although PEO interactions with water are less favorable as temperature increases, [57] the changes of the slope can only be explained by the presence of the VPTT of PNIPAM. The fixed temperature of the VPTT observed at both pH = 2 and 7.8, confirms that the [PNIPAM+PAA]/PBA BCDN was both temperature and pH responsive, without any mutual interference.

To verify if the mechanical properties were reinforced by the DNBC architecture, rheological test were performed on water swollen hydrogels (Figure S5). The storage modulus increased from 185 kPa for PNIPAM hydrogel to $E'_{[PNIPAM+PAA]/PBA} = 460$ kPa for BCDN hydrogel.

Addition of PBA and the hydrophilic double network in DNBC materials led thus to mechanical reinforcement.

3.3. Drug Loading and Drug Release ability.

To further evaluate the ability of the BCDN structures to act as drug carriers, we performed, as a proof of concept, the kinetic study of the release of acetyl salicylic acid (ASA), the active ingredient of Aspirin®. ASA has a characteristic absorbance peak at 275 nm. From the Beer-Lambert law, we could easily evaluate the concentration of ASA in solution as a function of its absorbance by UV-Visible spectroscopy, after having established a calibration curve (Figure S6 and S7). ASA is a relatively polar drug, which concentrates in the hydrophilic part of the synthesized hydrogels. The effects of temperature and pH on the release of ASA should, thus, be straightforward to observe.

Before loading the hydrogels with ASA, we first insured that any soluble fraction contained in the hydrogels was removed by performing Soxhlet extraction with THF. The drug loading was carried out by immersing ca. 0.2 g of the material in an ethanol solution of ASA ([ASA] = 150 g/L). Ethanol is a good solvent for ASA and swells the hydrophilic domains of the hydrogel. The weight ratio of loaded ASA was calculated from the weight difference on the dried samples before and after immersion (Figure 9).

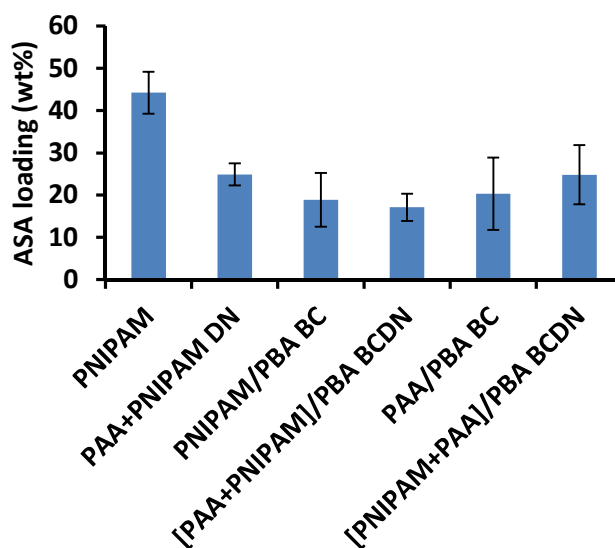


Figure 9: acetylsalicylic acid (ASA) loading of different materials.

The single PNIPAM network displayed the highest ASA loading ability of 44wt%. The high loading of PNIPAM was favored by a high swelling in water (>500wt %) or ethanol (700 wt%) compared to the other materials (<300 wt% with water and <400 wt% with ethanol). DN, BC or BCDN could still be loaded with 17 to 25 wt% of ASA, without any specific tendency. This proportion was higher than the typical proportion of active ingredient (few percent) commonly reported in pharmaceutical formulation.[58]

The effects of the pH (Figure 10A), temperature and tortuosity of the bicontinuous structure (Figure 10B) on the drug release have first been studied independently of each other. To perform this study, ASA was loaded into PNIPAM single network, PAA+PNIPAM double network and PNIPAM/PBA BC and the drug release experiments were carried out in water under the different conditions reported in the Figure 10. The cumulative weight percentage of ASA expelled from the material was calculated from the proportion of ASA released in water with a UV titration at 275 nm.

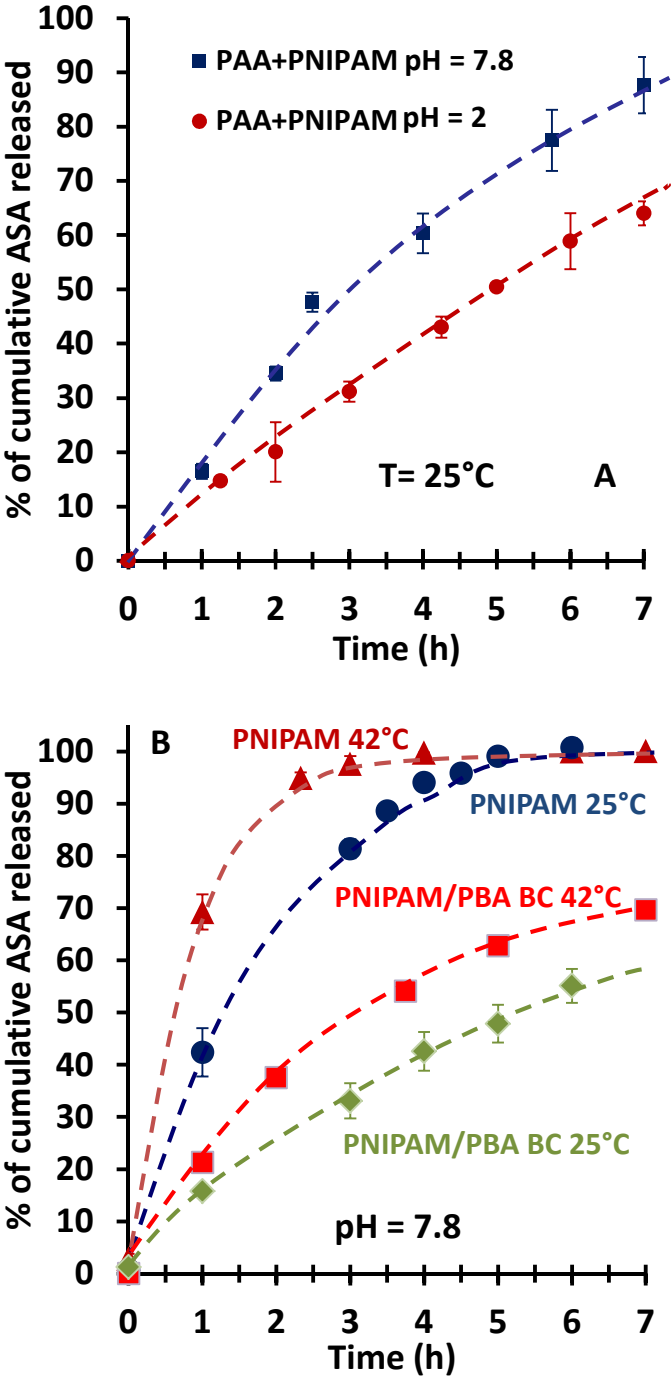
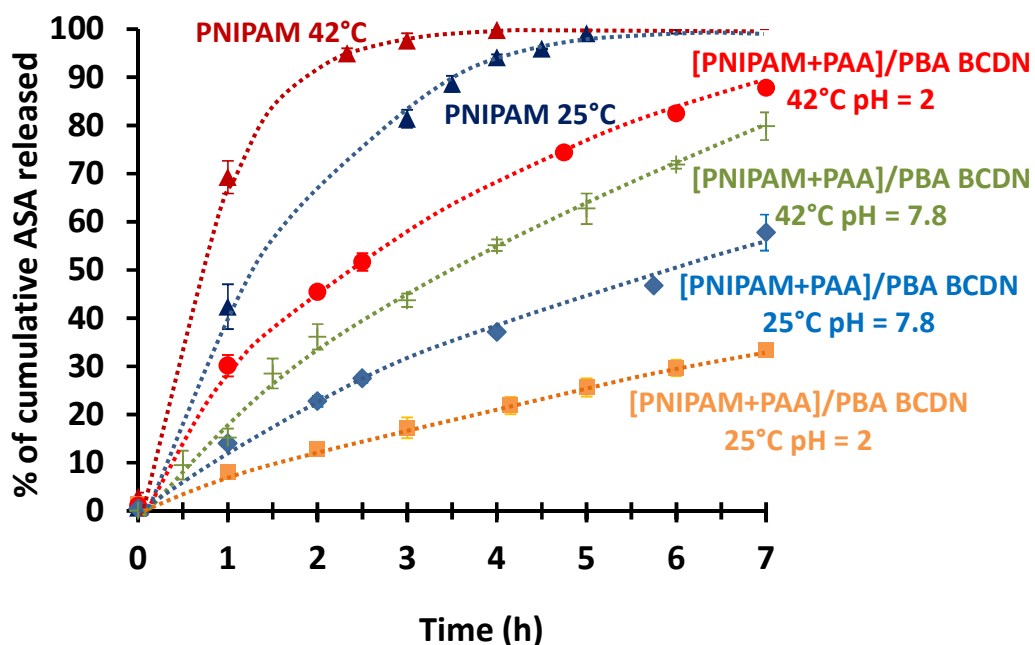


Figure 10: Effects of (A) pH and (B) temperature and tortuosity of the bicontinuous structure on the drug release. (The dash lines are used as guide eyes)

Figure 10A, shows the effect of pH on the cumulative release of ASA as a function of time, for the double network (not templated with the microemulsion) PNIPAM+PAA at 25°C. The drug was released much faster when the PAA was in the ionized state, with an open structure that does not prevent ASA from diffusing in the solution. The effect of temperature is shown in Figure 10B, where the evolution of the cumulative percentage of ASA released as a function of time for PNIPAM and PNIPAM/PBA bicontinuous network was plotted. The experiment was carried out in water at 25°C and at 42°C. Those temperatures were arbitrary selected (and kept along this study) well below and above the PNIPAM VPTT to show how the shrinkage of the PNIPAM network affects the release of ASA. As expected, ASA release is faster at 42°C than at 25°C because the collapsed state greatly favored the expulsion of the encapsulated molecules (Figure 1A). These two independent experiments confirmed that the release rate of ASA could be enhanced by the contraction of PNIPAM when T increased or when the PAA was in the ionized state ($\text{pH} \geq 5$).

The tortuosity effect on the drug delivery could also be observed in Figure 10B. The cumulative ratio of released ASA from the PNIPAM/PBA BC material was half that of the PNIPAM single network independently of the temperature. The PNIPAM confinement in the bicontinuous network reduced the exchange surface and thus slowed down the drug delivery. The hydrophobic polymer played the role of *in situ* created transport barriers.[16]

The most important results are shown in Figure 11, where the drug release properties of [PNIPAM+PAA]/PBA BCDN are reported. We performed this study in 4 different conditions, setting the pH to be equal to either 2 or 7.8, and at $T = 25$ or 42°C. Table 3 summarizes the conformation of the stimuli responsive polymers inside the BCDN material in these conditions and the impact on the drug release.



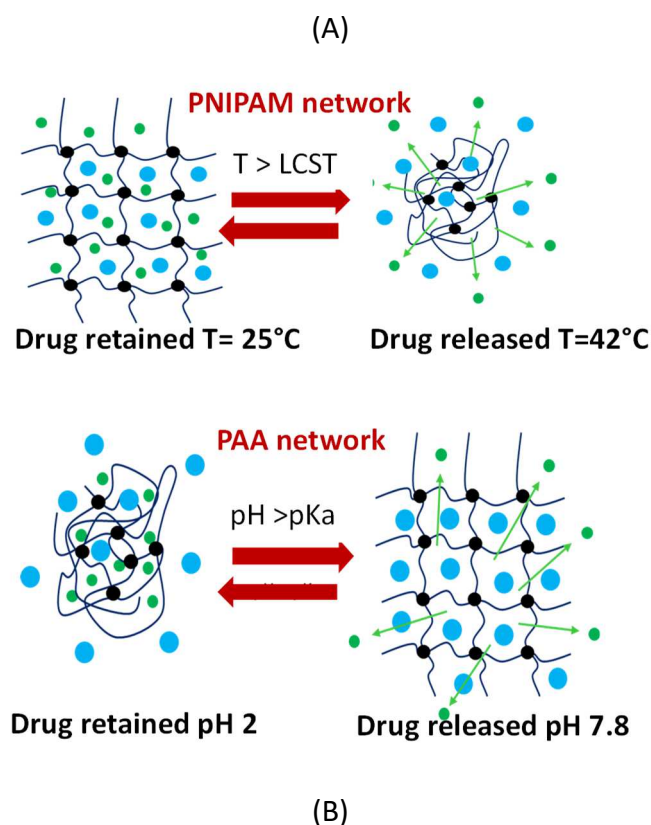


Figure 11: (A) Acetylsalicylic acid (ASA) release from pH and temperature sensitive [PNIPAM+PAA]/PBA BCDN material (The dash lines are used as guide eyes and release from PNIPAM are reported from figure 10 for comparison) and (B) scheme of the drug release according to the response polymer network concerned.

	pH= 2 T= 42°C	pH= 7.8 T= 42°C	pH= 7.8 T= 25°C	pH=2 T= 25°C
PAA conformation	collapsed (-)	swollen (+)	swollen (+)	collapsed (-)
PNIPAM conformation	collapsed (+)	collapsed (+)	swollen (-)	swollen (-)
Initial drug release rate (wt%/h)	30	18	11	5.7
Drug release tendency	↗↗	↗	↘	↘↘

Table 3: Summary of the polymer conformation and the impact on the drug release when promoted it is noted (+) and delayed noted (-) and the experimental drug release speed as function of pH and temperature conditions.

ASA was released from [PNIPAM+PAA]/PBA BCDN much slower than from the PNIPAM single network for all the temperature and pH tested, which confirmed that the tortuosity of the network strongly affected the drug delivery. The fastest release kinetic of ASA was observed at 42°C and pH = 2 (red circles). In these conditions up to 88% of the drug was released after 7 hours of annealing. The [PNIPAM+PAA]/PBA BCDN is a very interesting system since it combines the tortuosity imposed by the microemulsion templated polymerization with the presence of two hydrophilic networks that can have opposite effects on the drug release kinetic. For example, at 42°C and pH = 2 (red circles), both the PNIPAM and PAA networks

within the BCDN **were** in the collapsed state. According to their respective drug delivery mechanism (sketches in Figure 11) PNIPAM network **avored** the drug released, while the PAA prevented it. Since PNIPAM **was** the major component of the BCDN (49 wt%), it **had** the greatest influence on the drug delivery.

When the release of ASA **was** measured at 42°C, and pH = 7.8 (green crosses), PNIPAM **was** collapsed and the PAA network **was** extended. As a consequence, one would expect both effects to facilitate the expulsion of the drug and drastically increase its release kinetic. However, the drug release **was** slower in these conditions than at 42°C and pH = 2 (red circles). To better understand this result, one has to remember that in the double network architecture, the networks are in close vicinity of each other and the extended conformation of the PAA network is limited by the collapsed state of the predominant PNIPAM network. This effect **resulted** in an experimental initial drug release rate that decreased from 30 to 18 wt% per hour. Nevertheless, after 7 hours of annealing, the amount of ASA released **was** ca. 80 wt%, a value relatively close to that of the previous experimental conditions, i.e. 88 wt%. By fixing the pH at 7.8 and decreasing the temperature from 42 to 25°C (below the VPTT of PNIPAM, blue diamonds), the release rate **decreased** from 18 to 11 wt% per hour, only reaching 55 wt% after 7 hours. Even if the carboxylic acid functions **were** deprotonated with the PAA network in extended conformation promoting the drug release, the temperature **was** below the VPTT of PNIPAM, which **was** in an extended hydrophilic conformation and **delayed** the ASA release. The slowest drug release rate **was** observed at 25°C, temperature below the VPTT of PNIPAM, and at pH = 2, pH below the pKa of PAA (orange squares). The initial rate **dropped** to 5.7 wt% per hour and after 7h only 33 wt% of the drug **was** released. Both networks **adopted** a conformation that **retained** the drug, with a collapsed conformation for PAA (minor component) and extended conformation of PNIPAM (major component).

To conclude, with the [PNIPAM+PAA]/PBA BCDN developed in this study, one has an excellent control of the drug release from 88 wt% after 7 hours at 42°C pH = 2, 80 wt% at 42°C pH = 7.8, 58 wt% at 25°C pH = 7.8 and even 33 wt% at 25°C pH = 2. Contrary to PNIPAM, this material does not show a burst release behavior, i.e. less than 90% of ASA was released within 2-3 hours, which is actually favorable for considering future clinical studies. The release profiles are reported on the 7 first hours when the curves differences **were** meaningful. However for all experiments performed with the [PNIPAM+PAA]/PBA BCDN, the release of ASA **was** complete after 24h.

4. Conclusion

In this work, we have reported the synthesis a new type of hydrogel: a bicontinuous double network (BCDN). As a proof of concept, we performed preliminary tests on the drug release ability of this new system using ASA as the drug at different temperature and pH conditions.

To prepare this hydrogel, a hydrophobic monomer in water, a hydrophilic monomer and a surfmer were mixed at a specific ratio, to obtain a Winsor IV emulsion. *In situ*

polymerization/cross-linking of the system led to the formation of a bicontinuous network. While this structure has already been reported,[16] it has never been used as a template for the generation of a second hydrophilic network. By choosing the appropriate hydrophilic monomers (namely AA and NIPAM), we could prepare a pH and thermo-responsive BCDN. The hydrophilic and the hydrophobic phase bicontinuous templating was verified with thermomechanical analysis and microscopy.

The double network synthesized inside the hydrophilic phase led to the formation of a material with a particular molecular architecture that prevented the two stimuli responsive networks to interfere with each other. We also found that the BCDN showed limited water uptake compared to a single network or co-network. In addition the mechanical properties of the BCDN were considerably enhanced compared to that of single hydrogels.

The key parameter to design a BCDN with pH and temperature sensitivity was the order of formation of the hydrophilic networks. The best stimuli responsive BCDN was obtained when PAA/PBA bicontinuous template was formed first, followed by the synthesis of the PNIPAM network inside the hydrophilic phase of the template. This approach led to the formation of highly temperature responsive hydrogel containing *ca.* 49% of PNIPAM, 6% of PAA, 12 % of PBA and 33% of surfmer. Despite the relatively low amount of PAA, the BCDN also possessed noticeable pH responsive properties.

The preliminary tests of drug release, using acetylsalicylic acid as a drug model, were carried out on [PNIPAM+PAA]/PBA BCDN at different pHs and temperatures and the drug release kinetic profiles were monitored by UV-VIS. These experiments showed that the tortuosity induced by the bicontinuous template slowed down the desorption of the encapsulated molecules by reducing the surface area of the hydrophilic phase, containing the drug, with the aqueous medium. The [PNIPAM+PAA]/PBA BCDN combined both thermal and pH-sensitivity without shifting the VPTT. We believe that this type of material can be considered as drug carriers for on demand drug delivery. It could deliver drugs at concentrations above an effective threshold, at the targeted site for an extended period of time. As an oral medication, it could by-pass the low pH gastric acid barrier because the release was minimum at pH = 2. This study gives the proof of concept that an amphiphilic material sensitive to thermal and pH stimuli can be used as drug carrier for on-demand release, and paves the way toward studies of more hydrophobic drugs release such as current anticancer drugs.[59]

SUPPORTING INFORMATION.

AUTHOR INFORMATION

Corresponding Author

* E-mail: cedric.vancaeyzeele@u-cergy.fr

ORCID:

Cédric Vancaeyzeele: 0000-0002-9748-1562

Frédéric Vidal: 0000-0001-9803-0918

Gérald Guérin: 0000-0003-4997-0561

Clément Bombonnel: 0000-0002-5729-4391

NOTES

The authors declare no competing financial interest.

ACKNOWLEDGMENT

The authors would like to thank the project SESAME (Comicer project) supported by “Ile de France” region that has allowed the acquisition of confocal laser scanning microscope and the project SESAME (Cerasem project) supported by “Ile de France” region the acquisition of ZEISS Gemini SEM 300.

REFERENCES

- [1] Q. Chen, H. Chen, L. Zhu, J. Zheng, Fundamentals of double network hydrogels, *J. Mater. Chem. B.* 3 (2015) 3654–3676. doi:10.1039/C5TB00123D.
- [2] J. LANGER, ROBERT; FOLKMAN, Polymers for the sustained release of proteins and other macromolecules, *Nature.* 263 (1976) 797–800.
- [3] L.H. Fu, C. Qi, M.G. Ma, P. Wan, Multifunctional cellulose-based hydrogels for biomedical applications, *J. Mater. Chem. B.* 7 (2019) 1541–1562. doi:10.1039/c8tb02331j.
- [4] S.W. Bae, Y.H.; Okano, T.; Kirn, on Off Thermocontrol.Pdf, *Pharm Res.* 8 (1991) 624–628. doi:10.1023/A:1015860824953.
- [5] V. Alzari, D. Nuvoli, S. Scognamillo, M. Piccinini, E. Gioffredi, G. Malucelli, S. Marceddu, M. Sechi, V. Sanna, A. Mariani, Graphene-containing thermoresponsive nanocomposite hydrogels of poly(N-isopropylacrylamide) prepared by frontal polymerization, *J. Mater. Chem.* 21 (2011) 8727–8733. doi:10.1039/c1jm11076d.
- [6] M. Constantin, S. Bucatariu, V. Harabagiu, I. Popescu, P. Ascenzi, G. Fundueanu, Poly(N-isopropylacrylamide-co-methacrylic acid) pH/thermo-responsive porous hydrogels as self-regulated drug delivery system Paper dedicated to the 65th anniversary of “petru Poni” Institute of Macromolecular Chemistry of Romanian Academy, Iasi, Romania., *Eur. J. Pharm. Sci.* 62 (2014) 86–95. doi:10.1016/j.ejps.2014.05.005.
- [7] M. Karg, I. Pastoriza-Santos, B. Rodriguez-González, R. Von Klitzing, S. Wellert, T. Hellweg, Temperature, pH, and ionic strength induced changes of the swelling behavior of PNIPAM-poly(allylactic acid) copolymer microgels, *Langmuir.* 24 (2008) 6300–6306. doi:10.1021/la702996p.
- [8] S. Sun, J. Hu, H. Tang, P. Wu, Spectral interpretation of thermally irreversible recovery of poly(N-isopropylacrylamide-co-acrylic acid) hydrogel, *Phys. Chem. Chem. Phys.* 13 (2011) 5061. doi:10.1039/c0cp01939a.

- [9] J.P. Gong, Y. Katsuyama, T. Kurokawa, Y. Osada, Double-network hydrogels with extremely high mechanical strength, *Adv. Mater.* 15 (2003) 1155–1158. doi:10.1002/adma.200304907.
- [10] J.-Y. Sun, X. Zhao, W.R.K. Illeperuma, O. Chaudhuri, K.H. Oh, D.J. Mooney, J.J. Vlassak, Z. Suo, Highly stretchable and tough hydrogels, *Nature*. 489 (2012) 133–136. doi:10.1038/nature11409.
- [11] J.P. Gong, Why are double network hydrogels so tough?, *Soft Matter*. 6 (2010) 2583–2590. doi:10.1039/b924290b.
- [12] Z. Li, J. Shen, H. Ma, X. Lu, M. Shi, N. Li, M. Ye, Preparation and characterization of pH- and temperature-responsive nanocomposite double network hydrogels, *Mater. Sci. Eng. C*. 33 (2013) 1951–1957. doi:10.1016/j.msec.2013.01.004.
- [13] J. Shen, N. Li, M. Ye, Preparation and characterization of dual-sensitive double network hydrogels with clay as a physical crosslinker, *Appl. Clay Sci.* 103 (2015) 40–45. doi:10.1016/j.clay.2014.11.006.
- [14] M.K. Yoo, Y.K. Sung, Y.M. Lee, C.S. Cho, Effect of polyelectrolyte on the lower critical solution temperature of poly(N-isopropyl acrylamide) in the poly(NIPAAm-co-acrylic acid) hydrogel, *Polymer (Guildf)*. 41 (2000) 5713–5719. doi:10.1016/S0032-3861(99)00779-X.
- [15] Y.Y. Li, H.Q. Dong, K. Wang, D.L. Shi, X.Z. Zhang, R.X. Zhuo, Stimulus-responsive polymeric nanoparticles for biomedical applications, *Sci. China Chem.* 53 (2010) 447–457. doi:10.1007/s11426-010-0101-4.
- [16] C. Vancaeyzeele, F. Olivier, G. Petroffe, S. Peralta, F. Vidal, Nanostructured Thermal Responsive Materials Synthesized by Soft Templating, *ACS Appl. Mater. Interfaces*. 9 (2017) 12706–12718. doi:10.1021/acsami.7b00028.
- [17] S. Bourcier, C. Vancaeyzeele, F. Vidal, O. Fichet, Microemulsion as the template for synthesis of interpenetrating polymer networks with predefined structure, 54 (2013) 4436–4445. doi:10.1016/j.polymer.2013.05.067.
- [18] F. Candau, M. Pabon, J.-Y. Anquetil, Polymerizable microemulsions: some criteria to achieve an optimal formulation, *Colloids Surfaces A Physicochem. Eng. Asp.* 153 (1999) 47–59. doi:10.1016/S0927-7757(98)00425-7.
- [19] C. Stubenrauch, R. Tessendorf, R. Strey, I. Lynch, K. a Dawson, Gelled polymerizable microemulsions. 1. Phase behavior., *Langmuir*. 23 (2007) 7730–7. doi:10.1021/la700685g.
- [20] C. Stubenrauch, R. Tessendorf, A. Salvati, D. Topgaard, T. Sottmann, R. Strey, I. Lynch, Gelled polymerizable microemulsions. 2. Microstructure., *Langmuir*. 24 (2008) 8473–82. doi:10.1021/la800918g.
- [21] S. Kawano, D. Kobayashi, S. Taguchi, M. Kunitake, T. Nishimi, Construction of Continuous Porous Organogels, Hydrogels, and Bicontinuous Organo/Hydro Hybrid Gels from Bicontinuous Microemulsions, *Macromolecules*. 43 (2010) 473–479. doi:10.1021/ma901624p.
- [22] L.M. Gan, T.D. Li, C.H. Chew, W.K. Teo, L.H. Gan, Microporous Polymeric Materials from Polymerization of Zwitterionic Microemulsions, *Langmuir*. 11 (1995) 3316–3320. doi:10.1021/la00009a009.
- [23] C.H. Chew, L.M. Gan, L.H. Ong, K. Zhang, T.D. Li, T.P. Loh, P.M. MacDonald, Bicontinuous Structures of Polymerized Microemulsions: ¹H NMR Self-Diffusion and Conductivity Studies, *Langmuir*. 13 (1997) 2917–2921. doi:10.1021/la9607971.
- [24] C.H. Chew, T.D. Li, L.H. Gan, C.H. Quek, L.M. Gan, Bicontinuous-Nanostructured Polymeric Materials from Microemulsion Polymerization, *Langmuir*. 14 (1998) 6068–6076. doi:10.1021/la970990a.
- [25] J. Liu, L.M. Gan, C.H. Chew, W.K. Teo, L.H. Gan, Nanostructured Polymeric Materials from Microemulsion Polymerization Using Poly(ethylene oxide) Macromonomer, *Langmuir*. 13 (1997) 6421–

6426. doi:10.1021/la970640o.

- [26] P.Y. Chow, C.H. Chew, C.L. Ong, J. Wang, G. Xu, L.M. Gan, Ion-Containing Membranes from Microemulsion Polymerization, 33 (1999) 3202–3205.
- [27] C.L. Ong, L.M. Gan, C.K. Ong, H.S.O. Chan, G. Xu, Unusual Ionic Behavior in Microemulsion-Polymerized Membranes, *J. Phys. Chem. B.* 103 (1999) 7573–7576. doi:10.1021/jp990977u.
- [28] W. Xu, K. Siow, Z. Gao, S. Lee, P. Chow, L. Gan, Microporous Polymeric Composite Electrolytes from Microemulsion Polymerization, (1999) 4812–4819.
- [29] L.H. Sperling, Interpenetrating Polymer Networks: an overview, in: L.A. Sperling L.H.; Klemptner, D.; Utracki (Ed.), *Interpenetr. Polym. Networks.*, American Chemical Society Advances in chemistry series 239, Washington, DC, 1994: pp. 3–38.
- [30] C. Sager, Microemulsion Templating, in: V. Zvelindovsky (Ed.), *Nanostructured Soft Matter Exp. Theory, Simul. Perspect.*, 2007: pp. 3–44.
- [31] P.A. Winsor, Hydrotropy, solubilisation and related emulsification processes, *Trans. Faraday Soc.* 44 (1948) 376. doi:10.1039/tf9484400376.
- [32] R.H. and S.W.K. You Han Bae, Teruo Okano, Thermo-sensitive polymers as on-off switches for drug release, *Macromol. Rapid Commun.* 8 (1987) 481–485. doi:10.1016/j.diabres.2012.02.001.
- [33] J.N. Weinstein, Liposomes in the diagnosis and treatment of cancer, in: M.J. Ostro (Ed.), *Liposomes from Biophys. to Ther.*, Marcel Dekker, Inc., New York, 1987: pp. 40–101.
- [34] R. Yoshida, K. Sakai, T. Okano, Y. Sakurai, Pulsatile drug delivery systems using hydrogels, *Adv. Drug Deliv. Rev.* 11 (1993) 85–108. doi:10.1016/0169-409X(93)90028-3.
- [35] L.M. Ensign, R. Cone, J. Hanes, Oral drug delivery with polymeric nanoparticles: The gastrointestinal mucus barriers, *Adv. Drug Deliv. Rev.* 64 (2012) 557–570. doi:10.1016/j.addr.2011.12.009.
- [36] D.F. Evans, G. Pye, R. Bramley, A.G. Clark, T.J. Dyson, J.D. Hardcastle, Measurement of gastrointestinal pH profiles in normal ambulant human subjects, *Gut.* 29 (1988) 1035–1041. doi:10.1136/gut.29.8.1035.
- [37] D.C. Coughlan, F.P. Quilty, O.I. Corrigan, Effect of drug physicochemical properties on swelling/deswelling kinetics and pulsatile drug release from thermoresponsive poly(N-isopropylacrylamide) hydrogels, *J. Control. Release.* 98 (2004) 97–114. doi:10.1016/j.jconrel.2004.04.014.
- [38] T. Okano, Y.H. Bae, H. Jacobs, S.W. Kim, Thermally on-off switching polymers for drug permeation and release, *J. Control. Release.* 11 (1990) 255–265. doi:10.1016/0168-3659(90)90138-J.
- [39] A.K. Bajpai, S.K. Shukla, S. Bhanu, S. Kankane, Responsive polymers in controlled drug delivery, *Prog. Polym. Sci.* 33 (2008) 1088–1118. doi:10.1016/j.progpolymsci.2008.07.005.
- [40] C. Noirjean, C. Vancaeyzeele, S. Bourcier, F. Testard, F. Vidal, D. Carriere, O. Fichet, Nanostructure Changes upon Polymerization of Aqueous and Organic Phases in Organized Mixtures, *Langmuir.* 32 (2016) 10104–10112. doi:10.1021/acs.langmuir.6b02626.
- [41] F. Yan, J. Texter, Capturing nanoscopic length scales and structures by polymerization in microemulsions, *Soft Matter.* 2 (2006) 109. doi:10.1039/b513914g.
- [42] K.A. Page, D. England, J. Texter, Capturing Nanoscale Structure in Network Gels by Microemulsion Polymerization, *ACS Macro Lett.* 1 (2012) 1398–1402. doi:10.1021/mz300521d.
- [43] P. Fernandez, V. André, J. Rieger, A. Kühnle, Nano-emulsion formation by emulsion phase inversion, *Colloids Surfaces A Physicochem. Eng. Asp.* 251 (2004) 53–58. doi:10.1016/j.colsurfa.2004.09.029.

- [44] D. Rickert, A. Lendlein, A.M. Schmidt, S. Kelch, W. Roehlke, R. Fuhrmann, R.P. Franke, In vitro cytotoxicity testing of AB-polymer networks based on oligo(ϵ -caprolactone) segments after different sterilization techniques, *J. Biomed. Mater. Res.* 67B (2003) 722–731. doi:10.1002/jbm.b.10069.
- [45] C. Wischke, A.T. Neffe, S. Steuer, E. Engelhardt, A. Lendlein, AB-polymer Networks with Cooligoester and Poly(n-butyl acrylate) Segments as a Multifunctional Matrix for Controlled Drug Release, *Macromol. Biosci.* 10 (2010) 1063–1072. doi:10.1002/mabi.201000089.
- [46] J. Cui, K. Kratz, B. Hiebl, F. Jung, A. Lendlein, Soft poly(n-butyl acrylate) networks with tailored mechanical properties designed as substrates for in vitro models, *Polym. Adv. Technol.* 22 (2011) 126–132. doi:10.1002/pat.1816.
- [47] A.W. Long, S.; Clarke, S.; Davies, M.C.; Lewis, A.L.; Hanlon, G.W.; Lloyd, Controlled biological response on blends of a phosphorylcholine-based copolymer with poly(butyl methacrylate), *Biomaterials.* 24 (2003) 4115–4121. doi:10.1016/S0142-9612(03)00272-2.
- [48] Y. Sun, J. Collett, N.J. Fullwood, S. Mac Neil, S. Rimmer, Culture of dermal fibroblasts and protein adsorption on block copolymers of poly(butyl methacrylate-block-(2,3 propandiol-1-methacrylate-stat-ethandiol dimethacrylate)), *Biomaterials.* 28 (2007) 661–670. doi:10.1016/j.biomaterials.2006.09.024.
- [49] B. Bertolotti, H. Messaoudi, L. Chikh, C. Vancaeyzeele, S. Alfonsi, O. Fichet, Stability in alkaline aqueous electrolyte of air electrode protected with fluorinated interpenetrating polymer network membrane, *J. Power Sources.* 274 (2015) 488–495. doi:10.1016/j.jpowsour.2014.10.059.
- [50] P. Interpenetrating, P. Networks, *Interpenetrating Polymer Networks*, American Chemical Society, Washington, DC, 1994. doi:10.1021/ba-1994-0239.
- [51] C. Vancaeyzeele, O. Fichet, J. Laskar, S. Boileau, D. Teyssié, Polyisobutene/polystyrene interpenetrating polymer networks: Effects of network formation order and composition on the IPN architecture, 2006. doi:10.1016/j.polymer.2006.01.026.
- [52] V. Castellino, E. Acosta, Y.-L. Cheng, Interpenetrating polymer networks templated on bicontinuous microemulsions containing silicone oil, methacrylic acid, and hydroxyethyl methacrylate, *Colloid Polym. Sci.* 291 (2012) 527–539. doi:10.1007/s00396-012-2741-8.
- [53] L.H. Sperling, V. Mishra, The Current Status of Interpenetrating Polymer Networks, *Polym. Adv. Technol.* 7 (1996) 197–208. doi:10.1002/(SICI)1099-1581(199604)7:4<197::AID-PAT514>3.0.CO;2-4.
- [54] K. Aramaki, K. Tawa, L.K. Shrestha, T. Iwanaga, M. Kamada, Formation and Cleansing Performance of Bicontinuous Microemulsions in Water/Poly (oxyethylene) Alkyl Ether/Ester-Type Oil Systems, *J. Oleo Sci.* 62 (2013) 803–808. doi:10.5650/jos.62.803.
- [55] M. Whinton, T.C. Hughes, S. Peng, M.A. Brook, Silicone Microemulsion Structures Are Maintained During Polymerization with Reactive Surfactants, *Langmuir.* 34 (2018) 4374–4381. doi:10.1021/acs.langmuir.8b00240.
- [56] J.J. Maurer, D.J. Eustace, C.T. Ratcliffe, Thermal characterization of poly(acrylic acid), *Macromolecules.* 20 (1987) 196–202. doi:10.1021/ma00167a035.
- [57] E.E. Dormidontova, Role of Competitive PEO–Water and Water–Water Hydrogen Bonding in Aqueous Solution PEO Behavior, *Macromolecules.* 35 (2002) 987–1001. doi:10.1021/ma010804e.
- [58] K. Hörmann, A. Zimmer, Drug delivery and drug targeting with parenteral lipid nanoemulsions — A review, *J. Control. Release.* 223 (2016) 85–98. doi:10.1016/j.jconrel.2015.12.016.
- [59] A. Raval, S.A. Pillai, A. Bahadur, P. Bahadur, Systematic characterization of Pluronic® micelles and their application for solubilization and in vitro release of some hydrophobic anticancer drugs, *J. Mol. Liq.* 230 (2017) 473–481. doi:10.1016/j.molliq.2017.01.065.

Table of Contents /Abstract Graphic:

